Figure S1

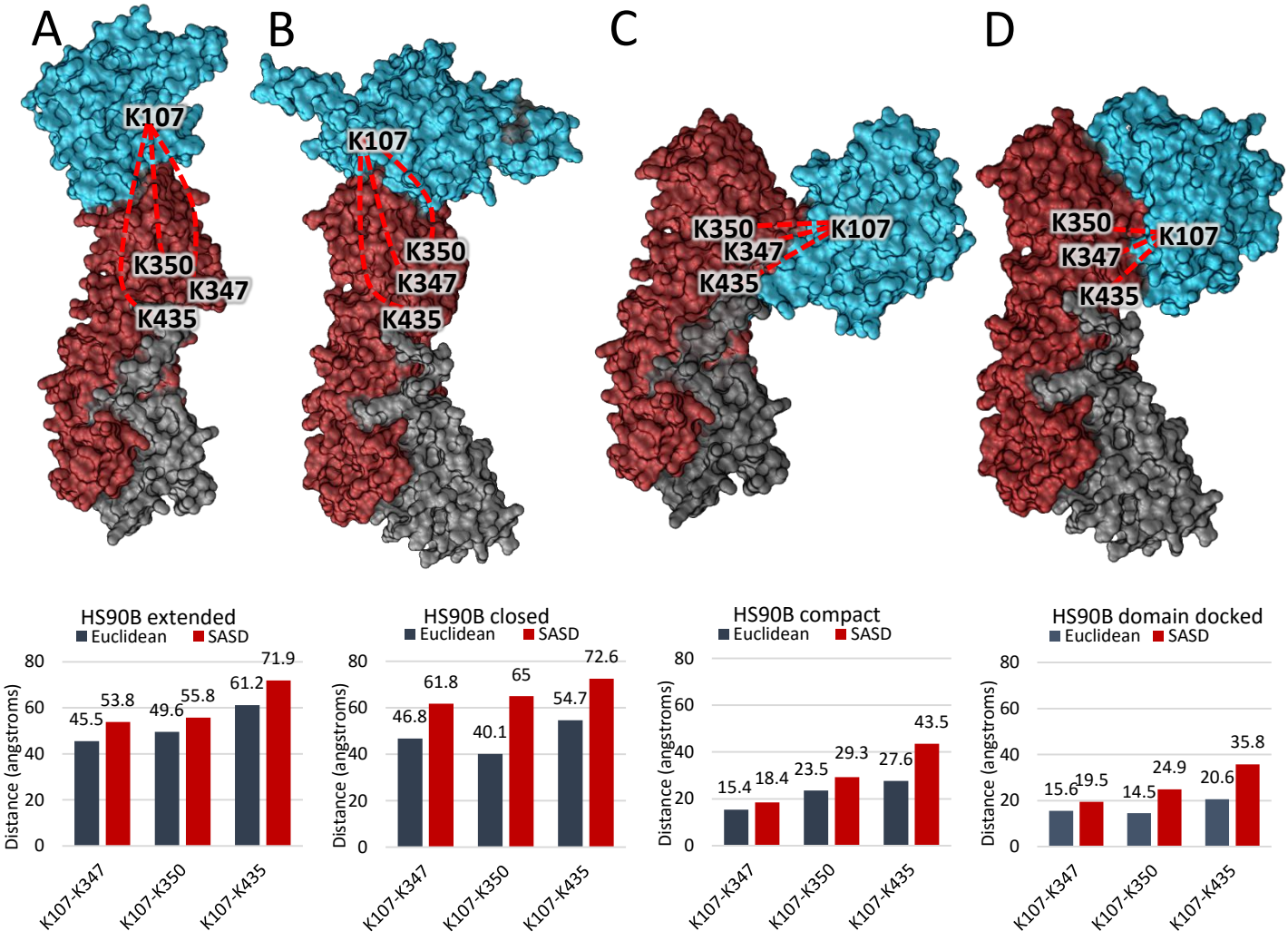

Figure S1. Related to Figure 2. Models of Hsp90 conformations. **(A)** Model of the extended conformation of HS90B generated by homology modeling using the extended model of *E. coli* HtpG[1] as a template. Cross-linked residues between the NTD and MD that increased with 17-AAG treatment are indicated by red space filling residues. **(B)** Closed model of HS90B generated by homology modeling using the PDB structure 2CG9 for the *S. cerevisiea* Hsp90 as a template. **(C)** Compact model of HS90B generated by homology modeling using the compact model of *E. coli* HtpG[1] as a template. **(D)** Model of HS90B generated by docking the NTD to the MD using observed inter-domain cross-links as distance constraints. The bar plot located below each model displays the Euclidean Cα-Cα distances as well as the solvent accessible surface distances (SASD) for the three cross-links between the NTD and MD that were observed with increased levels with 17-AAG treatment.

Figure S2

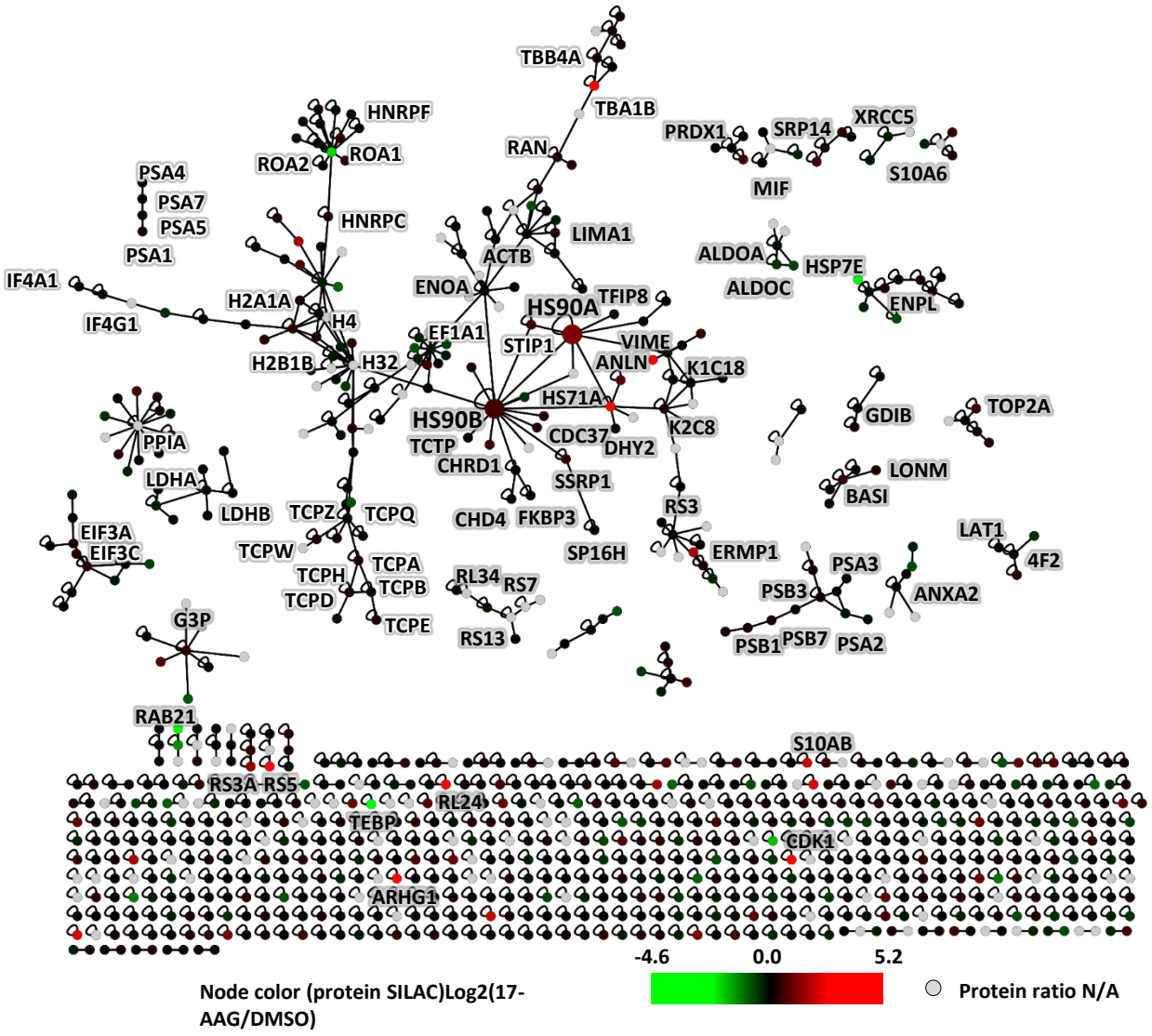

Figure S2. Related to Figure 4. Quantitative protein interaction network.
Protein level interaction network generated by quantitative cross-linking with mass spectrometry. The network consists of 893 nodes representing non-redundant cross-linked proteins, connected by 1042 edges representing one or more identified cross-links between or within proteins (3323 total cross-links, see Table S1). Selected protein nodes are labeled with their UniProt ID. A total of 783 cross-linked peptides originated from 176 proteins that are known Hsp90 interactors in the Picard database[2]. Nodes are colored according to the measured relative protein abundance between cells treated with 500 nM 17-AAG for 18hrs vs. DMSO control by global SILAC analysis. Grey nodes represent proteins for which no signal was obtained by global SILAC analysis. This network is available online at http://xlinkdb.gs.washington.edu/xlinkdb/ network name = ChavezChemBiol2016_BruceLab.

Figure S3

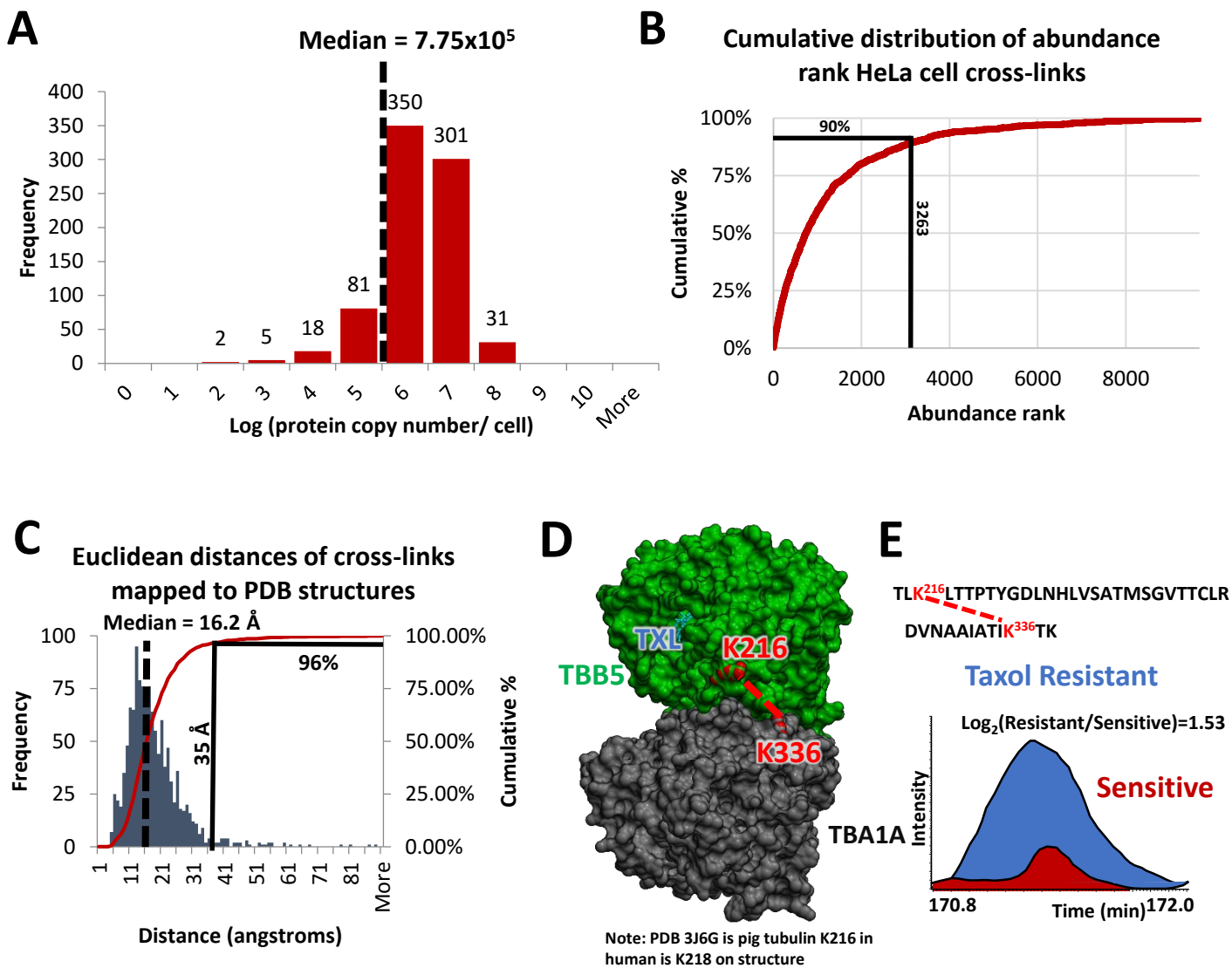

Figure S3. Related to Figure 4. Cross-linked peptide data compared with PDB and absolute protein abundance. (A) Distribution of cross-linked proteins mapped to absolute abundance levels[3]. **(B)** Cumulative protein abundance rank level for cross-linked proteins. Ninety percent of the cross-linked proteins were in the top 3263 most abundant proteins as measured by Kulak et al. **(C)** Distribution of Euclidean Cα-Cα distances for the 1245 cross-linked peptide pairs that could be mapped to existing structural data in the Protein Data Bank (PDB) (see **Table S3**). The remaining 2078 cross-linked peptides contained at least one residue without structural information in the PDB. The median distance of 16 angstroms agrees well with previous PIR cross-linking studies as well as large scale cross-linking studies carried out in other labs[4-6]. **(D)** Structure of the alpha-beta tubulin complex (PDB = 3J6G) with the cross-linked sites (K216 of beta tubulin (TBB5_HUMAN), and K336 of alpha tubulin (TBA1A_HUMAN)) indicated as red space filled residues. **(E)** Relative levels of the tubulin cross-linked peptide pair were increased in taxol resistant HeLa cells cultured in the presence of 10 nM taxol compared to normal HeLa cells treated with a DMSO control as indicated by the MS^1 level extracted ion chromatograms.

Figure S4

Figure S4. Related to Figure 5. Sequence alignment of HS90A and HS90B. Sequence alignment for HS90A and HS90B indicating the location of all lysine residues, those that were observed as cross-linked sites, and those residues that are known sites of posttranslational modification.

Figure S5

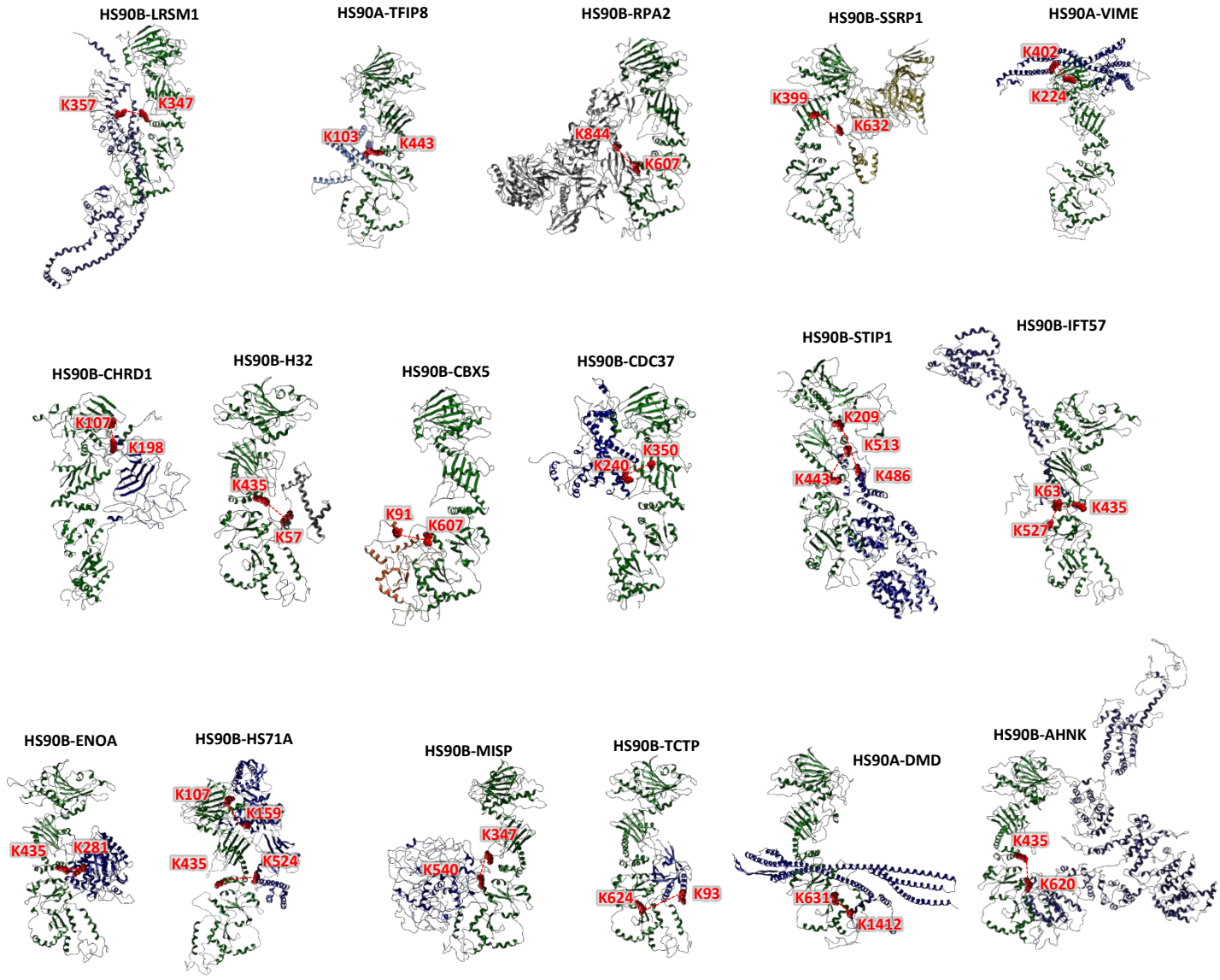

Figure S5. Related to Figure 5. Model structures for Hsp90 complexes. A total of 17 model complex structures were generated through cross-link distance constraint guided molecular docking for Hsp90 (green) and its interacting proteins (blue). Cross-linked lysine sites are shown as red space filled residues.

Figure S6

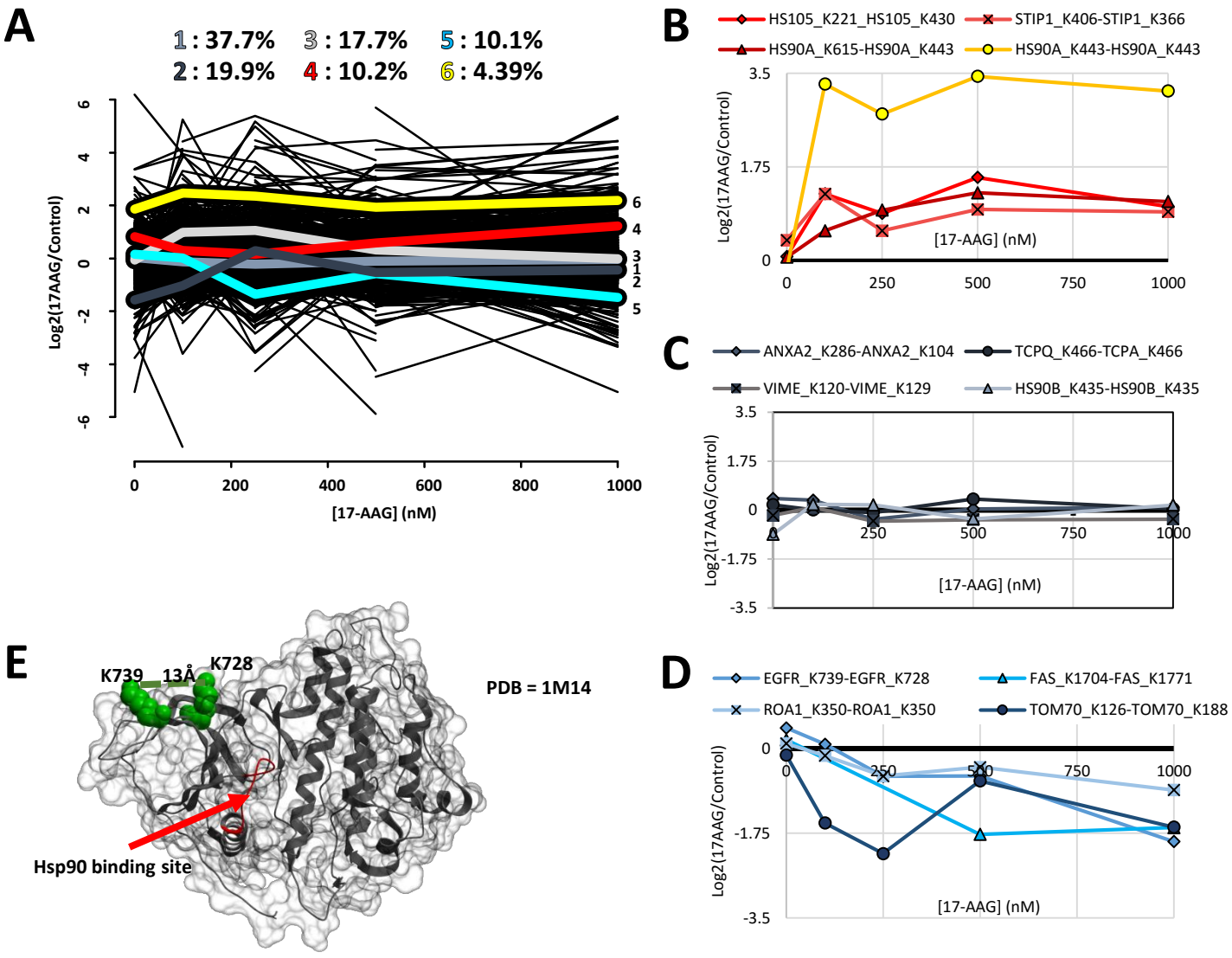

Figure S6. Related to Figure 6. Concentration of cross-linked peptides vary with 17-AAG treatment. **(A)** Plot of the Log_2(17-AAG/DMSO) values for 1505 cross-links as a function of 17-AAG concentration. The thick colored lines correspond to the mean trajectories resultant from K-means clustering analysis. **(B)** Selected examples of cross-linked peptides that displayed increased levels with increasing concentration of 17-AAG (clusters 4 & 6). These include a cross-link between the MD and CTD (K443-K615) of HS90A, a cross-link between TPR7 and TPR8 (K366-K406) of STIP1, a cross-link between K221 and K405 of heat shock protein 105 kDa (HS105) and the homodimer cross-link involving K443 of HS90A. **(C)** Selected examples of cross-linked peptides displaying no change in relative concentration with 17-AAG treatment. These include a cross-link between K104 and K206 of annexin A2 (ANXA2), a cross-link between K120 and K129 of vimentin (VIME), a cross-link between K466 of the TriC chaperonin complex proteins TCPA and K466 of TCPQ, and the HS90B homodimer cross-link involving K435. **(D)** Cross-linked peptides that displayed decreasing levels with increasing concentration of 17-AAG including K728-K739 of epidermal growth factor receptor (EGFR) which resides in close proximity to a known Hsp90 binding region[7] (**Supplementary Fig. 5**), a homodimer cross-link involving K350 of heterogeneous nuclear ribonucleoprotein A1 (ROA1), a cross-link between K1704 and K1771 of fatty acid synthase (FAS), and a cross-link between K126 and K188 of mitochondrial import receptor subunit TOM70 (TOM70). **(E)** Structure of EGFR (PDB = 1M14) with cross-linked sites K728 and K739 displayed as green space filled residues. The cross-linked peptide pair is proximal to an eight residue sequence (768-773, SVDNPHVC) known to be important for Hsp90 binding, and displayed decreasing levels with increasing concentration of 17-AAG, consistent with destabilization of EGFR upon Hsp90 inhibition.

Figure S7

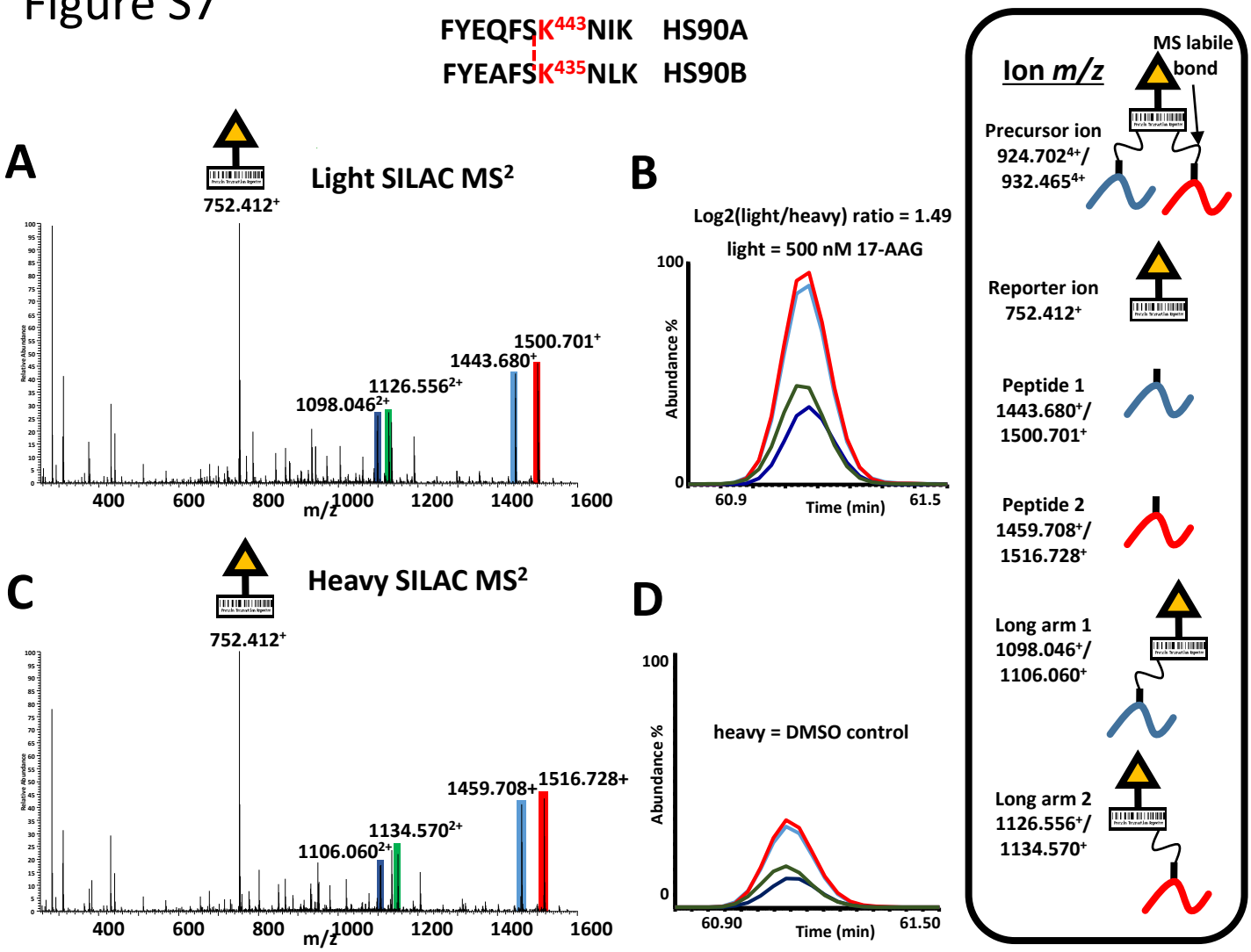

Figure S7. Related to Figure 6. Parallel reaction monitoring for quantification of cross-linked peptides. (A) MS^2 spectrum of the light isotope (m/z = 924.702^{4+}) cross-linked peptide pair linking K443 of HS90A with K435 of H(S90B. Fragment ions selected as PRM transitions used for quantification are indicated with colored bars. The ion at m/z = 1500.701^{+} (red) corresponds to the HS90A peptide (FYEQFS**K**^{443}NIK) with a PIR stump mass modification (197.032 Da) located on K443. The ion at m/z = 1443.680^{+} (light blue) corresponds to the HS90B peptide (FYEAFS**K**^{435}NIK) with a PIR stump mass modification (197.032 Da) located on K435. The ions at m/z = 1126.556^{2+} (green) and m/z = 1098.046^{2+} (dark blue) correspond to the HS90A and HS90B peptides containing a modification of 938.422 Da (PIR stump mass and reporter) at the cross-linked residues, resulting from the cleavage of a single labile bond in the PIR cross-linker. **(B)** Extracted ion chromatograms for the four fragment ion transitions indicated in **(A)** color coded accordingly. **(C)** MS^2 spectrum of the heavy isotope (m/z = 932.465^{4+}) cross-linked peptide pair linking K443 of HS90A with K435 of HS90B. The ion at m/z = 1516.728^{+} (red) corresponds to the isotopically heavy HS90A peptide (FYEQFS**K**^{443}NIK) with a PIR stump mass modification (197.032 Da) located on K443. The ion at m/z = 1459.708^{+} (light blue) corresponds to the isotopically heavy HS90B peptide (FYEAFS**K**^{435}NIK) with a PIR stump mass modification (197.032 Da) located on K435. The ions at m/z = 1134.570^{2+} (green) and m/z = 1106.060^{2+} (dark blue) correspond to the isotopically HS90A and HS90B peptides containing a modification of 938.422 Da (PIR stump mass and reporter) at the cross-linked residues. **(D)** Extracted ion chromatograms for the four fragment ion transitions indicated in **c** color coded accordingly. The figure legend on the right indicates the cartoon representations of the structures and measured m/z values for the ions selected as PRM transitions.

Supplemental Tables

Table S1. Related to Figures 2-7. Data for 3323 cross-linked peptide pairs identified from *in vivo* cross-linking in this study. Table includes information for all cross-linked peptide pairs identified from *in vivo* cross-linking of HeLa cells treated with varying concentrations (0-1000 nM) of 17-AAG.

Table S2. Related to Figure 3. Cross-linked peptide pairs identified by *in vitro* cross-linking of HS90B. Table includes information for 89 cross-linked peptide pairs that were identified from cross-linking purified HS90B *in vitro*.

Table S3. Related to Figures 2-5. 1245 cross-linked peptide pairs mapped to PDB structures. Table includes Euclidean Cα-Cα distances for 1245 cross-linked peptide pairs that were mapped to existing PDB structures (333 total PDB structures) using XLinkDB[8].

Supplemental Experimental Procedures

Cell culture

HeLa cells were seeded at a density of 5 x 10^6 cells into 150 mm culture dishes with 20 mL of SILAC DMEM medium containing either isotopically light L-lysine and L-arginine or isotopically heavy $^{13}C_6{}^{15}N_2$-L-lysine and $^{13}C_6$-L-arginine (Silantes) and supplemented with 10% dialyzed FBS (Valley Biomedical Inc.) and 1 % penicillin/streptomycin (Fisher Scientific). Cells were treated with various concentrations (100, 250, 500, 1000 nM) Tanespimycin (17-N-allylamino-17-demethoxygeldanamycin, 17-AAG) (Cayman Chemicals), 300 nM XL888 (Selleckchem), 400 μM Novobiocin (Sigma) or 0.1% v/v dimethyl sulfoxide (DMSO) for 18 h before harvesting from the plates with 5 mL of phosphate buffered saline (PBS) (Fisher Scientific) containing 5 mM EDTA. Cells were washed with PBS and pelleted by centrifugation at 300 g for 3 min. Cell pellets were then suspended in 170 mM Na_2HPO_4 pH 8.0 in preparation for chemical cross-linking.

Chemical cross-linking of SILAC cells

Isotopically light and heavy cells were mixed at equal numbers (2 x 10^7 cells) in biological replicates (duplicates of each treatment condition for a total of 10 biological samples), either light 17-AAG treated/ heavy control or light control/ heavy 17-AAG treated, before adding the PIR cross-linker (Biotin Aspartate Proline – N-hydroxyphthalamide, BDP-NHP), synthesized by solid phase peptide synthesis as previously described[9], from a concentrated stock solution (333 mM) in DMSO to a final concentration of 10 mM. PIR cross-linkers, initially described in 2005[10] and subsequently applied to *p. aeruginosa*[11], a. baumannii infection of human cells[12], and quantitative comparison of drug resistant cancer cells[4], rely on engineered labile bonds in the cross-linker that can be specifically cleaved in situ to release to intact peptide chains. Cleavage of these bonds during mass spectrometric analysis results in a predictable mass relationship which is exploited during LC-MS analysis as described in that specific section below. The reaction was carried out at room temperature for 1 h with constant mixing. The reaction time of 1 hr allows time for over 99 % of the cross-linker to react based on the measured half-life of 7.5 min. After 1 h the cells were pelleted by centrifugation at 300 g for 3 min the supernatant was removed and the cross-linking reaction was quenched by suspending the cell pellet in 0.1 M NH_4HCO_3 pH 8.0.

***In vitro* cross-linking of HS90B**

50 μg recombinant HS90B at a concentration of 1.1 mg/mL in 20mM TRIS, pH 7.5, containing 500 mM sodium chloride, 5% glycerol, and 1mM DTT (45 μL total) was obtained from Enzo (ADI-SPP-777-D). The volume was adjusted to 500 μL with 50 mM HEPES, 1 mM EDTA, 5 mM $MgCl_2$, 100 mM KCl and divided into two 250 μL aliquots. The samples were loaded onto 30 kDa molecular weight cutoff filters (Millipore) and washed 3 times w/250 μL HEPES buffer. After buffer exchange the protein was recovered and the sample volume was adjusted to 50 μL with HEPES buffer. To one sample, 500 nM 17-AAG was added, to the other an equivalent volume of DMSO and the samples were incubated on ice for 30 min. Chemical cross-linking was performed by adding 1 mM BDP-NHP and incubating at room temp for 1 h. The samples were then adjusted to 8 M urea, reduced with 5 mM tris(2-carboxyethyl)phosphine (TCEP) (Fisher Scientific) for 30 minutes followed by alkylation for 45 minutes with 10 mM iodoacetamide (Fisher Scientific). Samples were then digested overnight by incubating at 37°C with a 1:100 ratio of trypsin to protein. Peptide samples were acidified to pH 2 with formic acid before desalting by solid phase extraction using C18 Sep-Pak cartridges (Waters). Desalted samples were concentrated by vacuum centrifugation using an EZ2-Plus evaporator (Genevac). Samples were then resuspended in 25 μL 0.1% formic acid and stored at -80°C until LC-MS analysis.

Cell lysis and cross-linked peptide sample preparation

Cross-linked cells were lysed by suspending the cell pellet in ice cold 8 M urea solution in 0.1 M tris buffer pH 8.0. Sample viscosity was reduced by sonication using a GE – 130 ultrasonic processor, followed by reduction and alkylation of cysteine residues by incubation with 5 mM TCEP for 30 minutes followed by a 45 minute incubation with 10 mM iodoacetamide (Fisher Scientific). To reduce the urea concentration to less than 1 M the samples were diluted by a factor of 10 with fresh 0.1 M tris buffer pH 8.0. The protein concentration was measured using the Pierce Coomassie protein assay (Thermo). Samples containing 10 mg of total protein were enzymatically

digested by adding a 1:200 ratio of sequencing grade modified trypsin (Promega) to protein and incubating at 37°C for 18 hrs. Peptide samples were acidified to pH 2 with formic acid before desalting by solid phase extraction using C18 Sep-Pak cartridges (Waters). Desalted samples were concentrated by vacuum centrifugation using an EZ2-Plus evaporator (Genevac). Peptide samples were then adjusted to a volume of 0.5 mL with 7 mM KH_2PO_4, 30% acetonitrile pH 2.8 before being fractionated by strong cation exchange chromatography (SCX) using an Agilent 1200 series HPLC system equipped with a 250 x 10.0 mm column packed with Luna 5 µm 100 Å particles (Phenomenex). Peptide separation was accomplished using a binary mobile phase solvent system consisting of solvent A (7 mM KH_2PO_4, 30% acetonitrile pH 2.8) and solvent B (7 mM KH_2PO_4, 350 mM KCl, 30% acetonitrile pH 2.8) at a flow rate of 1.5 mL/min using the following gradient program: 0-7.5 min 100% A, 7.5-47.5 min 95% A/5% B to 40% A/ 60% B, 47.5-67.5 min 40% A/ 60% B to 100% B, 67.5-77.5 min 100% B, 77.5-97.5 min 100% A. A total of 15 fractions (5 min time slices, 7.5 mL each) were collected starting after an initial 17.5 minute delay. Resulting SCX fractions were concentrated by vacuum centrifugation before their pH was adjusted to 8.0 by the addition of 0.1 M NH_4HCO_3. Fractions 6 and 7 were combined as well as fractions 11-14. To each of five fractions (6-7, 8, 9, 10, 11-14) 200 µL of monomeric avidin slurry (Thermo) was added and the samples were mixed for 30 minutes at room temperature. To remove non-biotin containing peptides the avidin beads were washed 3 x with 3 mL 100 mM NH_4HCO_3 pH 8.0 before eluting the cross-linked peptides by incubating the beads for five minutes each with two 500 uL aliquots of 70% acetonitrile, 30% H_20 containing 0.5 % formic acid. The enriched cross-linked peptide sample was then concentrated by vacuum centrifugation and stored at -80°C until LC-MS analysis.

LC-MS^n analysis of cross-linked peptide pairs

Samples containing PIR cross-linked peptides were analyzed in technical triplicate by liquid chromatography mass spectrometry using a Waters NanoAcquity UPLC coupled to a Thermo Velos-FTICR mass spectrometer[13] and a real-time adaptive, targeted mass spectrometry method developed for PIR cross-linked peptides[9]. Peptides were loaded onto a 3 cm x 100 µm inner diameter fused silica trap column packed with a stationary phase consisting of MichromMagic C8, 5 µm diameter, 200 Å pore size particles (Bruker) with a flow rate of 2 µL/min of mobile phase consisting of 98% solvent A (H_2O containing 0.1% formic acid) and 2% solvent B (ACN containing 0.1% formic acid) for 10 minutes. Peptides were then fractionated over a 60 cm x 75 µm inner diameter fused silica analytical column packed with Michrom Magic C8, 5 µm diameter, 100 Å pore size particles by applying a linear gradient from 95% solvent A, 5% solvent B to 60% solvent A, 40% solvent B over either 120 or 240 minutes at a flow rate of 300 nL/min. Eluting peptide ions were ionized by electrospray ionization by applying a positive 2 kV potential to a laser pulled spray tip at the end of the analytical column. The Velos-FTICR mass spectrometer was operated utilizing ReACT where ions with a charge state of four or greater were selected for high resolution MS^2 analysis in the ICR cell where an "on-the-fly" check of the observed fragment ion masses against the PIR mass relationship (Mass Precursor = Mass Reporter Ion + Mass Peptide 1 + Mass Peptide 2) is performed. Masses that satisfied the PIR relationship within a tolerance of 20 ppm mass error triggered subsequent low resolution MS^3 analyses of the released cross-linked peptide ions.

Parallel reaction monitoring quantification of cross-linked peptides

Samples containing PIR cross-linked peptides were analyzed using a targeted parallel reaction monitoring (PRM) method using an Easy-nLC (Thermo) coupled to a Q-Exactive Plus mass spectrometer (Thermo). Peptides were loaded onto a 3 cm x 100 µm inner diameter fused silica trap column packed with a stationary phase consisting of ReproSil C18, 5 µm diameter, 200 Å pore size particles (Dr. Maisch GmbH) with a flow rate of 2 µL/ min of mobile phase consisting of 98% solvent A (H_2O containing 0.1% formic acid) and 2% solvent B (ACN containing 0.1% formic acid) for 10 minutes. Peptides were then fractionated over a 60 cm x 75 µm inner diameter fused silica analytical column packed with ReproSil C18, 5 µm diameter, 100 Å pore size particles (Dr. Maisch GmbH) by applying a linear gradient from 95% solvent A, 5% solvent B to 60% solvent A, 40% solvent B over 120 minutes at a flow rate of 300 nL/min. Eluting peptide ions were ionized by electrospray ionization by applying a positive 2 kV potential to a laser pulled spray tip at the end of the analytical column. The Q-Exactive Plus mass spectrometer was operated using a PRM method targeting selected cross-linked peptides with the following parameters: Resolving power set to 17,500, AGC target set to 2e5 ions, maximum ion time set to 50 ms, isolation window of 3 m/z, normalized collision energy set to 25.

Identification and of quantification of cross-linked peptides

ReACT generated MS^3 spectra containing peptide fragmentation information were searched against a subset of the UniProt reference proteome database (downloaded 10.01.15) for Homo sapiens containing both forward and reverse protein sequences (7030 total sequences) using Comet[14] (v. 2015.01). The 3515 proteins included in the subset database were identified as putative PIR reactive proteins through a stage 1 database approach as previously described[4]. Comet search parameters included; a 20 ppm precursor mass tolerance, allowing for -1, 0, +1, +2, or +3 ^{13}C offsets, a 1.005 Da fragment ion mass tolerance with 0.4 Da offset, static modifications for the isotope labeled amino acids Arg-$^{13}C_6$ (6.020129 Da) and Lys-$^{13}C_6{}^{15}N_2$ (8.014199 Da) as well as carbamidomethylation of Cys (57.021464 Da), oxidation (15.9949 Da) on Met was added as a variable modification, and the BDP stump mass (197.0324 Da) on Lys was added as a required variable modification, considering only fully tryptic peptide sequences and allowing for up to 3 missed cleavage sites. False discovery of cross-linked peptides was addressed by searching a concatenated database containing forward and reverse protein sequences as previously described. Briefly, cross-linked peptide sequences were reported for cases where both peptide sequences contained an internal Lys residue modified by the cross-linker (197.0324 Da) and were assigned at < 5% false discovery rate using a forward/reverse database search strategy. The global FDR was estimated to be less than or equal to 1.5% and was measured by allowing

reverse peptide sequences that pass the 5% FDR threshold at the identification stage to be mapped to PIR relationships and taking the ratio of decoy cross-linked peptide pairs (either one or two reverse peptide sequences) to the total number of cross-linked peptide pairs.

Relative quantitative analysis of cross-linked peptide pairs between 17-AAG treated and DMSO control conditions was performed using MassChroQ[15]. Accurate mass and retention time information for the light isotope forms of each cross-linked peptide pair identified was input. Isotope shifts included Arg-$^{13}C_6$ (6.020129 Da) and Lys$^{13}C_6{}^{15}N_2$ (8.014199 Da). Retention time alignment was performed across replicates using the Obiwarp method. Quantification was performed using the area under the curve for extracted ion chromatograms for the MS1 signal from cross-linked peptide pair ions that were generated using a ppm tolerance of plus or minus 10 ppm using the Zivy peak detection algorithm.

For statistical analysis, peak areas output from MassChroQ were further analyzed using R. Log_2 ratios for 17-AAG/DMSO peak areas were calculated followed by median centering of the distribution of Log_2 ratios. For cross-linked peptides with multiple ratios, the standard deviation and 95% confidence interval was calculated. As we have previously demonstrated (Chavez et al., 2015), using SILAC based quantification it is generally possible to statistically distinguish fold changes of greater than two fold in cross-linked peptide pairs. K-means clustering of the 17-AAG titration data was accomplished using the R-package kml[16]. The R-pakage kml is a tool designed to work specifically on trajectories. It works by clustering correlated continuous variables, in this case Log_2 ratios for cross-linked peptides across 17-AAG concentration, into distinct groups of categorical variables. It employs a K-means hill climbing algorithm belonging to the expectation-maximization class. This works by initially assigning each observation to a cluster. The clusters are then optimized using an expectation phase in which the centers of each cluster are computed, followed by a maximization phase in which each observation is assigned to its nearest cluster. Alternation of the two phases are repeated until no further changes occur in the clusters. The algorithm is able to deal with missing values, and is designed to be run several times with varying starting conditions and number of clusters to look for. Settings for kml included partitioning between 5 to 8 clusters, rerunning the clustering algorithm 40 times for each cluster number. Euclidean distance was used with mean centering and a starting condition of nearlyAll. Heat map images were generated with Java Treeview[17].

Molecular docking and complex model selection

For proteins cross-linked to Hsp90 without complete structural data in the PDB, Phyre2 was used in intensive modeling mode to generate full length structural models. One to one threading in Phyre2 was used to generate human Hsp90 conformer models from *E. coli* HtpG extended, closed and compact models[1]. PDB structures were used for proteins with complete crystal structures. Rigid body docking based on complimentary shape criteria was performed using Patchdock[18]. Patchdock was run with the following settings: Phyre2 models for HS90A or HS90B were input as the receptor while the interacting protein was input as the ligand. Clustering RMSD was set to 4 angstroms and complex type was set to default. Observed cross-links were input as distance constraints from 0-35 angstroms between the Ca atoms of the cross-linked lysine residues. For each complex the top 100 docking results were analyzed by an updated algorithm based on the R-package XLMap[19] called XLComplex, provided for free online at http://brucelab.gs.washington.edu/software.html

Supplemental References

1. Shiau AK, Harris SF, Southworth DR, Agard DA (2006) Structural Analysis of E. coli hsp90 reveals dramatic nucleotide-dependent conformational rearrangements. *Cell* **127:** 329-340

2. Echeverria PC, Bernthaler A, Dupuis P, Mayer B, Picard D (2011) An interaction network predicted from public data as a discovery tool: application to the Hsp90 molecular chaperone machine. *PLoS One* **6:** e26044

3. Kulak NA, Pichler G, Paron I, Nagaraj N, Mann M (2014) Minimal, encapsulated proteomic-sample processing applied to copy-number estimation in eukaryotic cells. *Nat Methods* **11:** 319-324

4. Chavez JD, Schweppe DK, Eng JK, Zheng C, Taipale A, Zhang Y, Takara K, Bruce JE (2015) Quantitative interactome analysis reveals a chemoresistant edgotype. *Nature communications* **6:**

5. Chavez JD, Weisbrod CR, Zheng C, Eng JK, Bruce JE (2013) Protein interactions, post-translational modifications and topologies in human cells. *Molecular & Cellular Proteomics* **12:** 1451-1467

6. Liu F, Rijkers DT, Post H, Heck AJ (2015) Proteome-wide profiling of protein assemblies by cross-linking mass spectrometry. *Nat Methods*, 10.1038/nmeth.3603

7. Ahsan A, Ray D, Ramanand SG, Hegde A, Whitehead C, Rehemtulla A, Morishima Y, Pratt WB, Osawa Y, Lawrence TS*, et al.* (2013) Destabilization of the epidermal growth factor receptor (EGFR) by a peptide that inhibits EGFR binding to heat shock protein 90 and receptor dimerization. *J Biol Chem* **288:** 26879-26886

8. Zheng C, Weisbrod CR, Chavez JD, Eng JK, Sharma V, Wu X, Bruce JE (2013) XLink-DB: database and software tools for storing and visualizing protein interaction topology data. *J Proteome Res* **12:** 1989-1995

9. Weisbrod CR, Chavez JD, Eng JK, Yang L, Zheng C, Bruce JE (2013) In vivo protein interaction network identified with a novel real-time cross-linked peptide identification strategy. *Journal of proteome research* **12:** 1569-1579

10. Tang X, Munske GR, Siems WF, Bruce JE (2005) Mass spectrometry identifiable cross-linking strategy for studying protein-protein interactions. *Anal Chem* **77:** 311-318

11. Navare AT, Chavez JD, Zheng C, Weisbrod CR, Eng JK, Siehnel R, Singh PK, Manoil C, Bruce JE (2015) Probing the Protein Interaction Network of Pseudomonas aeruginosa Cells by Chemical Cross-Linking Mass Spectrometry. *Structure* **23:** 762-773

12. Schweppe DK, Harding C, Chavez JD, Wu X, Ramage E, Singh PK, Manoil C, Bruce JE (2015) Host-Microbe Protein Interactions during Bacterial Infection. *Chem Biol*, 10.1016/j.chembiol.2015.09.015

13. Weisbrod CR, Hoopmann MR, Senko MW, Bruce JE (2013) Performance evaluation of a dual linear ion trap-Fourier transform ion cyclotron resonance mass spectrometer for proteomics research. *J Proteomics* **88:** 109-119

14. Eng JK, Hoopmann MR, Jahan TA, Egertson JD, Noble WS, MacCoss MJ (2015) A Deeper Look into Comet-Implementation and Features. *J Am Soc Mass Spectrom* **26:** 1865-1874

15. Valot B, Langella O, Nano E, Zivy M (2011) MassChroQ: a versatile tool for mass spectrometry quantification. *Proteomics* **11:** 3572-3577

16. Genolini C, Falissard B (2011) KmL: a package to cluster longitudinal data. *Comput Methods Programs Biomed* **104:** e112-121

17. Saldanha AJ (2004) Java Treeview--extensible visualization of microarray data. *Bioinformatics* **20:** 3246-3248

18. Schneidman-Duhovny D, Inbar Y, Nussinov R, Wolfson HJ (2005) PatchDock and SymmDock: servers for rigid and symmetric docking. *Nucleic Acids Res* **33:** W363-367

19. Schweppe DK, Chavez JD, Bruce JE (2015) XLmap: an R package to visualize and score protein structure models based on sites of protein cross-linking. *Bioinformatics*, 10.1093/bioinformatics/btv519